

FINITE ELEMENT MODELING OF THOR-LX AND ITS APPLICATION

Hyung Yun Choi

Joong Yub Shin

Hongik University

Korea

Inhyeok Lee

Hankook ESI

Korea

Chang Nam Ahn

Han Il Bae

Hyundai Motor Co. & KIA Motors Corp

Korea

Paper No. 05-0125

ABSTRACT

The first part of this paper introduces a FE modeling effort of the lower extremity of Thor dummy, Thor-Lx Hybrid III retrofit. The FE model consists of 9,800 nodes and 8,300 elements, of which 2,900 are deformable solid elements. Three kinematic ankle joint elements are respectively used to represent dorsiflexion, inversion/eversion, and internal/external rotation of the foot. In addition to kinematic joint elements which represent the initial linear resistance developed by continuous joint stop, sliding contact interfaces are also defined between neoprene rubber and rotating center blocks for the subsequent non-linear stage. This two-stage joint definition then provides the precise description of ankle joint characteristics both in loading and unloading phases. The simulated outcomes of FE model have been validated for the performance of the ankle under different rotation motions and showed good agreement with both quasi-static and dynamic test results.

The second part of the paper deals with a practical application of the FE Thor-Lx model. Numerical simulations of a NCAP frontal 40% offset crash with a small size sedan are performed. A sub-structuring scheme for isolating the occupant compartment from the full car crash simulation is then adopted in order to facilitate the parametric study in which the various levels of structural deformations are attempted. The FE model of Hybrid III 50th percentile male upper body including knees and femurs is utilized to mount Thor-Lx and Hybrid III leg for the quantitative and comparative analyses of both legs. The Hybrid III leg mostly produces higher tibia index values than Thor-Lx due to its simple ankle joint structure which might result in steep increase of moments at the end of the range of motion. The paper concludes with the improved capabilities of Thor-Lx for the injury risk assessment compared with Hybrid III leg.

INTRODUCTION

Crash injuries of the lower extremities are usually not fatal, but may result in long-term impairment and immobility. It has been estimated that annually about 110,000 occupants sustain lower limb injuries with a severity rating of 2 or 3 on the Abbreviated Injury Scale (AIS).[1] Almost half of these injuries occur below the knee and, of those, ankle and foot injuries are the most frequent and can be responsible for long-term impairment.[2,3] Accordingly, in 2002, NHTSA announced an ANPRM (Advanced Notice of Proposed Rulemaking, 49 CFR Part 572, Docket No. NHTSA 2002-11838) for including the instrumented lower legs in vehicle crash tests to assess the risk of injuries occur below the knee. In the NHTSA proposal, two kinds of dummy lower legs for addressing lower leg injuries in frontally-oriented impacts are proposed: (1) The Hybrid III/Denton (HIII/Denton) instrumented leg and (2) the more recently designed Thor-Lx Hybrid III Retrofit (Thor-Lx/HIIIr) leg. Only one of these two available lower leg designs would be incorporated into the safety standard after some comparative evaluation period. The Thor-Lx appears to have substantially improved ankle and tibia biofidelity and a broader set of instruments while the Denton leg has been used over many years by the automotive industry for vehicle development. Since its formal release in December of 2000, the design of Thor-Lx has been kept nearly unchanged and incorporated in Thor NT which is the latest version of Thor dummy.[4]

The objective of this study is to build a finite element model of Thor-Lx. The detail modeling procedures such as geometry construction, FE meshing, and material characterizations are introduced as well as the results of model validation. A practical application with the developed FE model, the assessment of lower leg injury due to toepan intrusion, is also presented in this paper.

FINITE ELEMENT MODELING OF THOR-LX

The geometry of the Thor-Lx FE model is based on the AutoCAD drawing package (version 3.2, downloaded from NHTSA website: http://www-nrd.nhtsa.dot.gov/departments/nrd-51/thor_LX/Thorlxweb.html). The 3D solid model in CATIA[5] format was then built by utilizing the drawing package. After the 3D solid modeling work had been completed, the finite element meshing was performed with HyperMesh[6] and converted into Pam-Crash[7] input format. Fig. 1 shows the CATIA solid model and the FE mesh of Thor-Lx model.

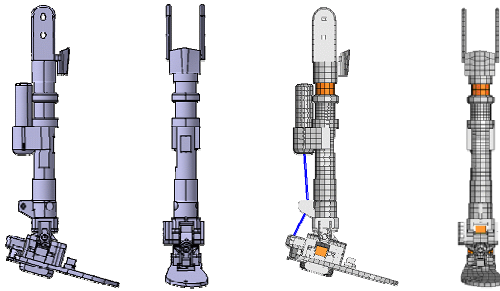
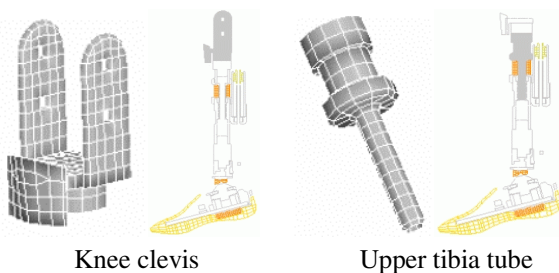


Fig. 1 Solid model (left 2) and FE mesh (right 2) of Thor-Lx model

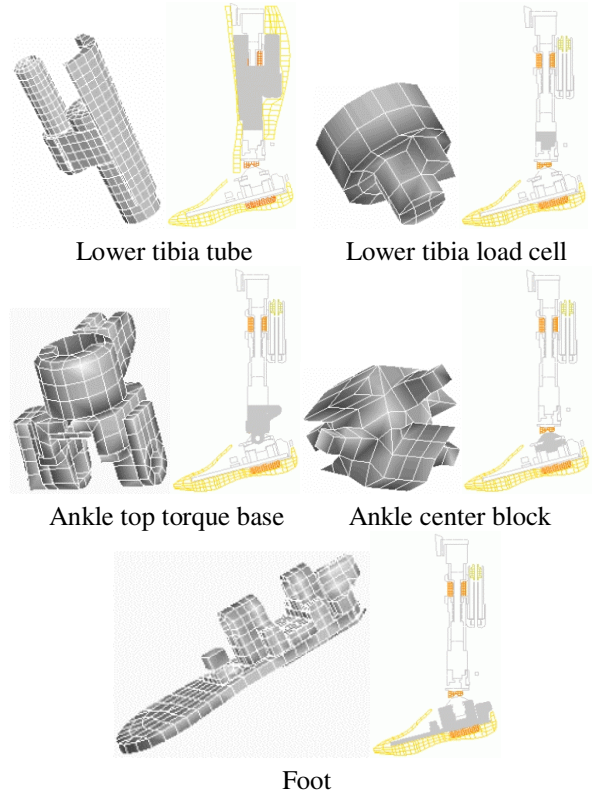
Rigid Body Definition

Most metal parts in the Thor-Lx model are rigidly modeled while the rubbers and urethanes are modeled as deformable materials. These rigid bodies are modeled by null shell elements (material type 100 in PAM-SAFE[7]). Dynamic properties such as mass and principle moments of inertia for each rigid body definition were calculated from the 3D solid model in CATIA. Fig. 2 shows the rigid bodies in the Thor-Lx model which are connected to each other by either deformable parts, kinematic joints for the ankle joint, or springs for the load cells.



Knee clevis

Upper tibia tube



Lower tibia tube

Lower tibia load cell

Ankle top torque base

Ankle center block

Foot

Fig. 2 Rigid body definitions in FE model

Deformable Part Definition

The rubber and urethane parts such as joint stops, tibia flesh, and heel pad were modeled by linear visco-elastic materials in which the characteristics were determined through the tuning processes with various component tests. The visco-elastic parameters of various deformable parts are listed in Table 1 and the corresponding figures are in Fig. 3.

Table 1 Visco-elastic parameters of various deformable materials in Thor-Lx model

Components	$K^{1)}$	$G_0^{2)}$	$G_\infty^{3)}$	$\beta^{4)}$
Tibia Compliant Bushing	0.28	4	1.4	0.5
Z-Rotation Stop	0.28	3.5	1.75	0.525
Dorsi-Plantar Flexion Soft Stop	0.09	20	4	0.085
Inversion-Eversion Soft Stop	0.079	3.5	0.7	0.85
Heel Pad	0.16	3.5	1.75	0.525
Foot Flesh	0.16	3.5	1.75	0.525

1) Bulk modulus (kN/mm^2)

2) Short time shear modulus (N/mm^2)

3) Long time shear modulus (N/mm^2)

4) Decay constant (sec^{-1})

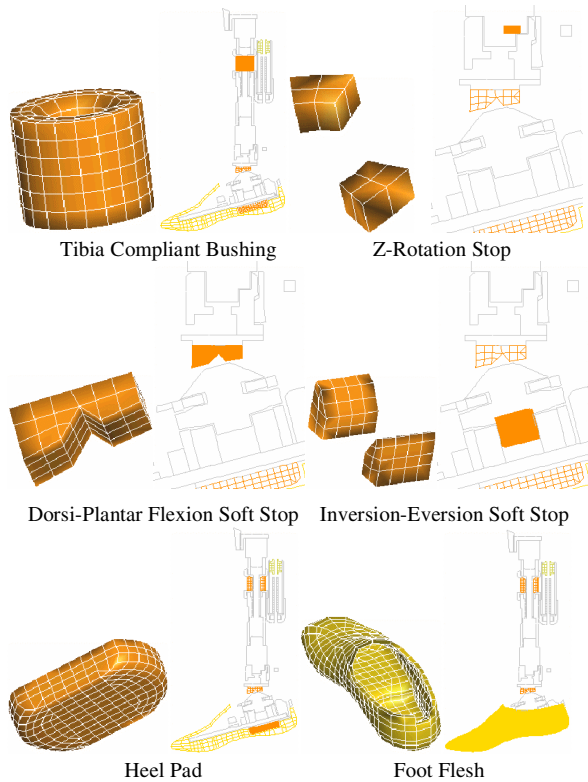


Fig. 3 Deformable parts in FE model

One of improved biofidelic characteristics of Thor-Lx compared with Hybrid III is the introduction of Achilles spring tube shown in Fig. 4 which consists of coil spring in parallel with elastomer spring element. In the model, nonlinear bar element was employed, and its loading/unloading characteristics are shown in Fig 5.

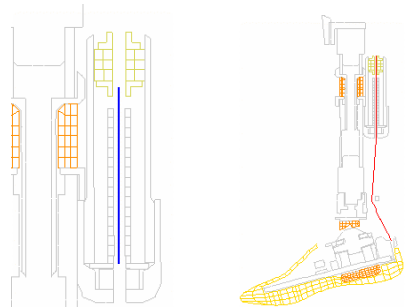


Fig. 4 Achilles spring tube and cable

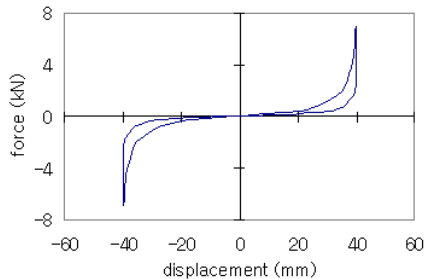


Fig. 5 Loading/unloading curve for Achilles spring

Kinematic Joint Definition

Ankle joint rotations about all three axes in Thor-Lx are independent of each other as shown Fig 6, and inversion/eversion (xversion) and dorsiflexion/plantarflexion (flexion) have separate, anatomically located centers of rotation. Flexion occurs primarily at the talar joint in the human, and xversion occurs at the subtalar joint. This is replicated in the Thor-Lx by placing the xversion joint 17 mm distal to the flexion joint. The first resistance of xversion and flexion is generated by the continuous joint stop (CJS) which increased its resistive torque in a linear fashion as the joint rotates. This first stage of linear joint resistance is modeled by a revolute joint element. Secondary resistance develops when the stopper begins to engage the rotating center block. In the modeling, the realistic geometry and characteristics of rubber block has been kept and a sliding interface definition between the center block and rubber element is applied to represent the second stage resistance in the joint. Fig. 7 shows a schematic of the joint features producing the two-stage resistance.

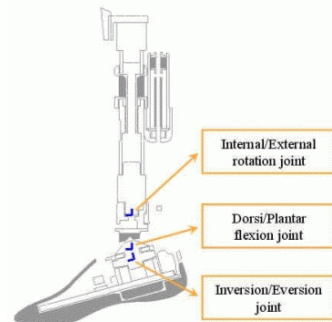


Fig. 6 Locations of ankle joints

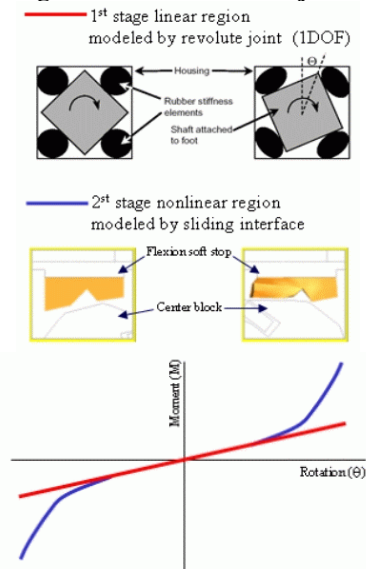


Fig. 7 Schematic joint characteristics representing two-stage resistance

Load Cell Definition

Load cells are defined in the model by using nonlinear 6 DOF spring elements. Each load cell is modeled by a single spring with zero length and is located at the intersection of the load cell's neutral axes. Fig. 8 shows the locations of load cells. They act stiff translational and rotational springs just for an accurate representation of reality. Although the physical load cells may be single, five or six axis transducers, load cells in the model provide all six output channels (i.e., three forces and three moments).

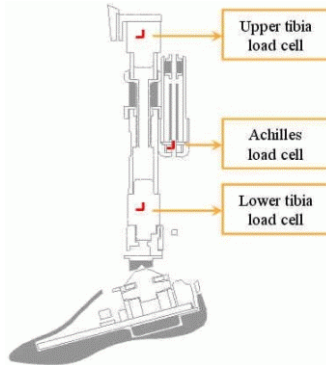


Fig. 8 Locations of load cells

VERIFICATION OF THE MODEL

In order to ensure the quality of the FE model, two kinds of validation were performed against the certification requirements and the design reference guidelines presented in NHTSA documents [8, 9].

Quasi-static ankle motion tests

The quasi-static ankle motion tests to examine the range of motion and resistance of the ankle joint soft stops in dorsiflexion/plantarflexion, inversion/eversion, and internal/external rotations were simulated according to the same test procedures as used in NHTSA certification procedures [9]. The simulated responses of the model were then compared with the test results.

Fig. 9 shows the set-up for the dorsiflexion test with and without Achilles. The detailed test and measurement procedures can be found in NHTSA certification procedures [9]. Simulation results with and without the Achilles cable are shown in Fig. 10 and 11, respectively. The simulated moment-angle curves in both cases coincide quite well with a typical response from the tests.

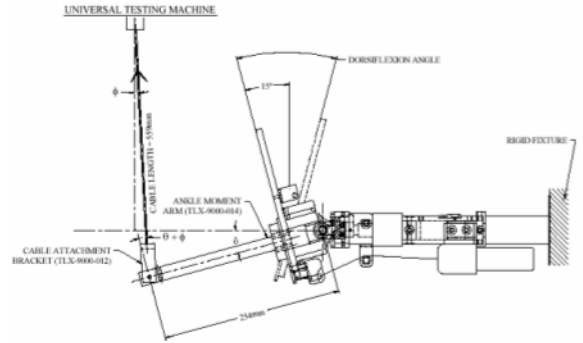


Fig. 9 Test set-up for quasi-static dorsiflexion test

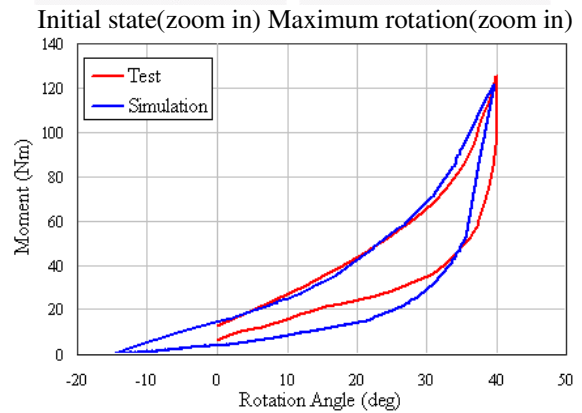
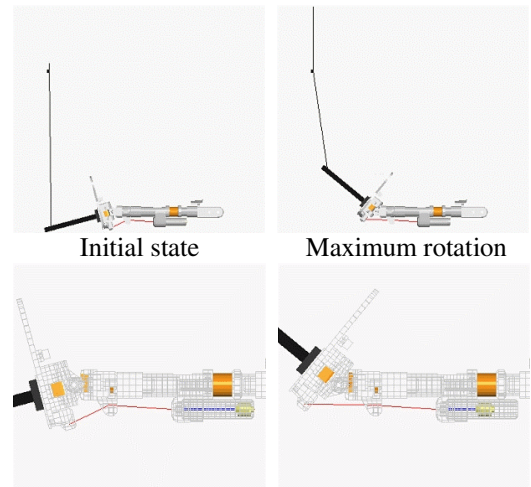
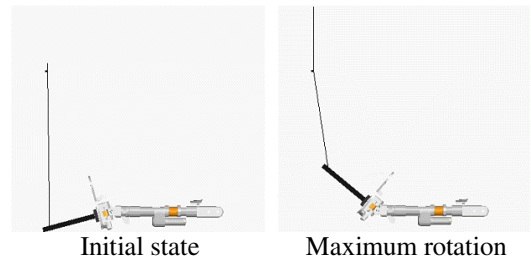


Fig. 10 Simulation of quasi-static dorsiflexion (with Achilles cable)



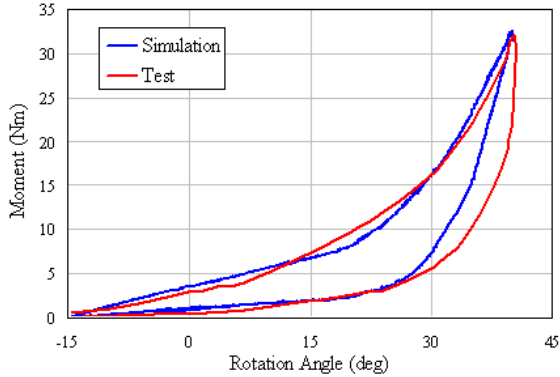


Fig. 11 Simulation of quasi-static dorsiflexion (without Achilles cable)

The test set-up and procedure for plantarflexion are similar to those for the dorsiflexion and the simulated moment-angle curve is presented in Fig. 12.

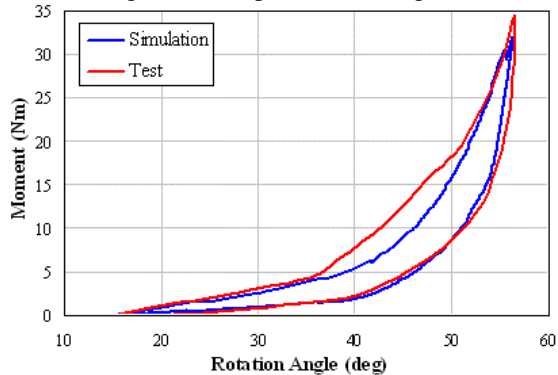


Fig. 12 Simulation of quasi-static plantarflexion

Fig. 13 shows a comparison between test and simulation results for inversion. Since the predicted unloading path of simulation is little higher than that of the test, the energy dissipation is also underestimated. Due to the symmetric design of the xversion joint, the validation for eversion had been skipped. The results of the simulation for the internal rotation compared with a test are shown in Fig. 14. The internal/external joint in the Thor-Lx was designed to provide approximate biofidelity within the range of $\pm 15^\circ$ and the considerable discrepancy in unloading path between simulation and test might have been caused by excessive rotation in the test and could be neglected.

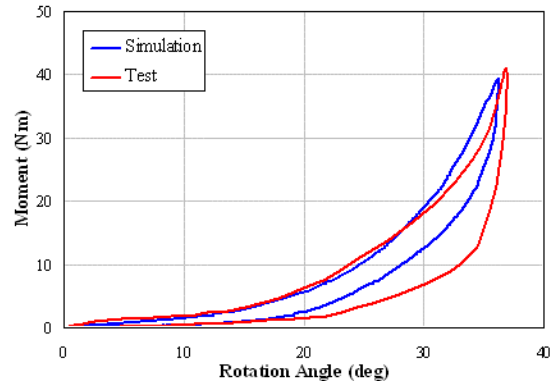


Fig. 13 Simulation of quasi-static inversion

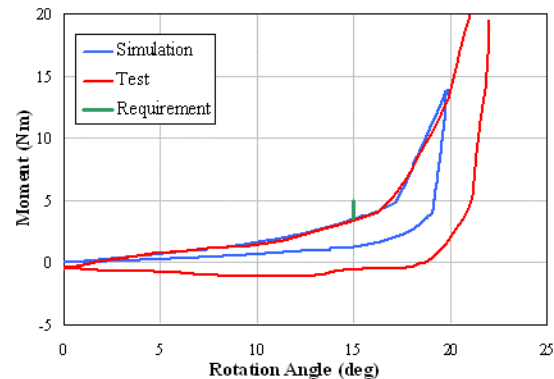
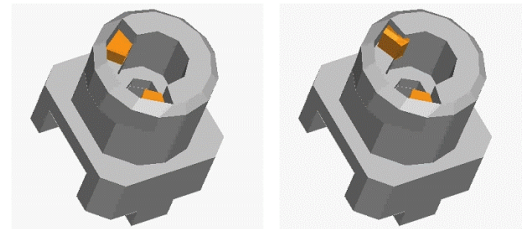


Fig. 14 Simulation of quasi-static internal rotation

Dynamic impact tests

To validate the dynamic performance of the ankle joint and the compliant elements in the foot and tibia, two pendulum impacts were simulated. The anatomical areas of pendulum impact are the ball of the foot and the heel of the foot. Test setups and the simulation results for impact simulations are presented from Fig. 15 to Fig. 18.

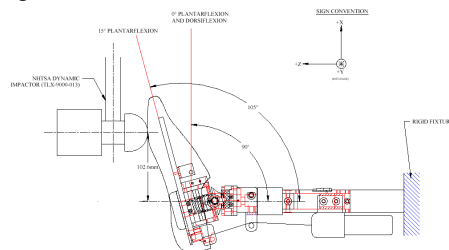
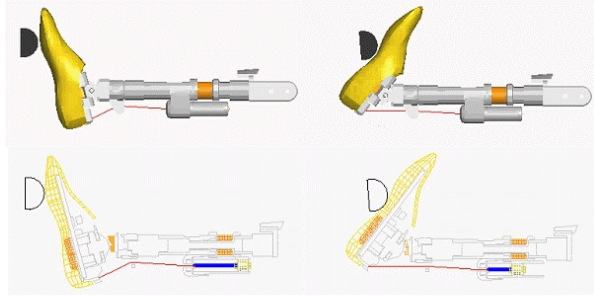


Fig. 15 Ball of foot impact set-up



Initial state Maximum rotation

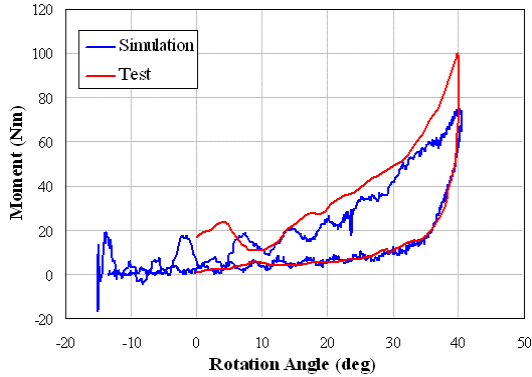


Fig. 16 Simulation result of ball of foot impact

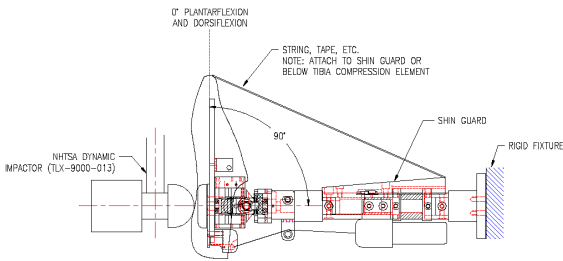
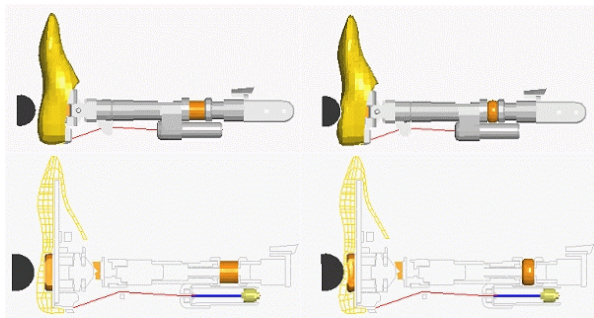


Fig. 17 Heel of foot impact set-up



Initial state Maximum compression

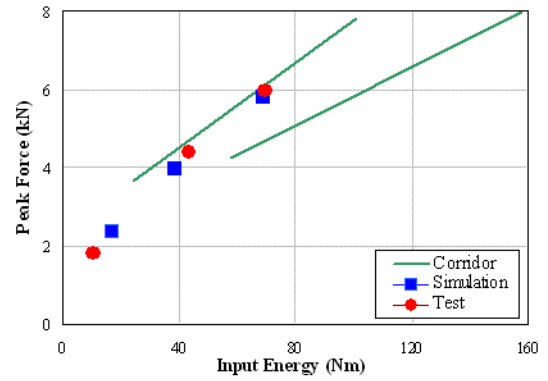


Fig. 18 Simulation result of heel of foot impact

ASSESSMENT OF LOWER EXTREMITY INJURY WITH THOR-LX

In order to examine the FE model of Thor-Lx for practical use, a series of crash simulations, NCAP 40% offset crash for a small size sedan have been performed using the Thor-Lx model. Translational and rotational vehicular deceleration pulses, and the deformation profile of occupant compartment computed from the full car simulation shown in Fig. 19, were applied to create an isolated offset sled model shown in Fig. 20. Applying a sub-structuring scheme to this offset sled model, a parametric study for various levels of structural deformation has been performed.

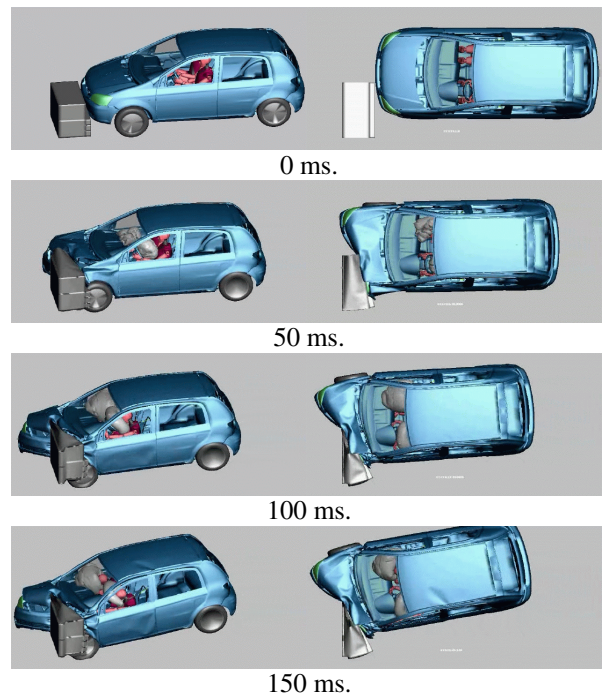


Fig. 19 Simulation of full car offset crash (Left: side view, Right: top view)

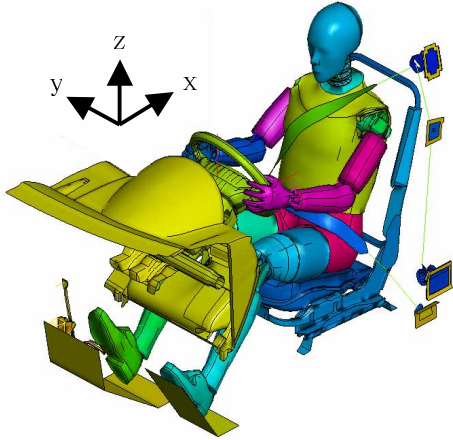


Fig. 20 Offset sled model

A finite element Hybrid III 50% dummy model developed by FTSS was adopted for an occupant surrogate in this study. The Thor-Lx model introduced in first part of this paper was also retrofitted to the Hybrid III thigh.

The intrusion profiles of the pedal and toe pan in the offset sled model were selected as design variables in parameter study. Three levels of severity for toe pan intrusion were fabricated and used for the quantitative investigation of their effects on lower extremity injury risk. The amount of intrusion of the toe pan and the floor in case #1 were adopted from the base NCAP 40% offset car crash simulation in Fig. 19. The overall amounts of intrusions were then raised for cases #2 and #3 as shown in Fig. 21 to mimic more excessive structural deformations. The intrusions in case #1 were from the deformation of the dash panel only while cases #2 and #3 were intended to represent the decreasing gap between the dash and the occupant due to floor collapse.

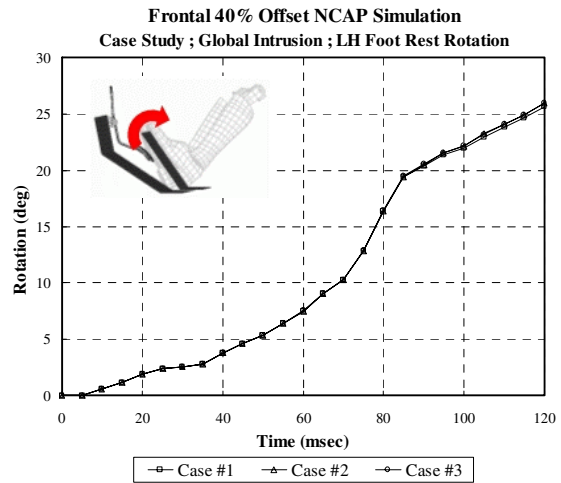
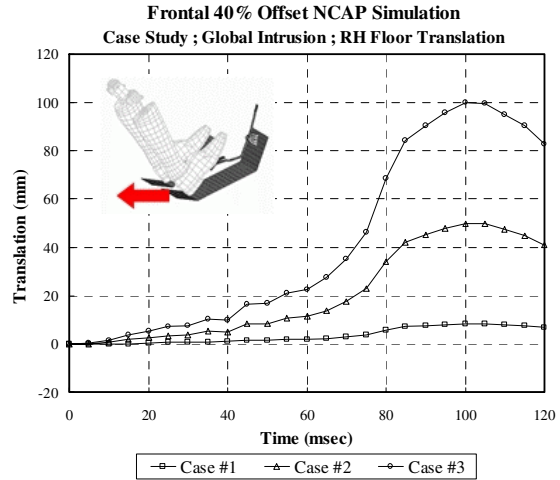
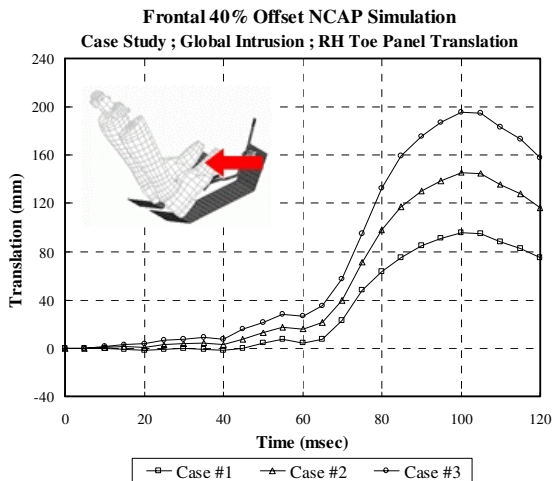


Fig. 21 Intrusion profiles in parametric study

Table 2 shows the injury predictions of the three cases in the parametric study. The amount of left dorsiflexion in the Thor-Lx showed small changes with increasing intrusion, which means the dorsiflexion had reached its maximum range due to the forward excursion of the body at an early stage. Therefore, RTI (Revised Tibia Index) and tibia F_z (axial force in tibia) for the Thor-Lx increased gradually with the intrusion due to the rise of ankle joint force and moment after the dorsiflexion had saturated. The Thor-Lx predicted more than a 50% risk of left side ankle joint injury for all three levels of intrusion severity. The highest severe tibia and fibula fracture risk predicted by the Thor-Lx was a 50% probability of fracture on the right hand side for case #3. The TI (Tibia Index) values of the Hybrid III exceeded the injury threshold for both sides in cases #2 and #3. The Hybrid III ankle tended to develop a very steep increase in the moment at its limit of rotation as shown in Fig. 22 because of its joint stop design, and thus the Hybrid III predicted relatively high risks of injury. The amounts of xversion (inversion and

eversion) for the Thor-Lx did not show a strong dependence on intrusion severity.

Table 2 Injury predictions from parametric study

Thor-Lx	Injury Limits		Case #1		Case #2		Case #3	
	25% Prob.	50% Prob.	Left	Right	Left	Right	Left	Right
Femur Fz	9.04 kN	11.15 kN	-1.46	2.82	-1.62	2.94	-2.09	5.76
Knee Shear	-	15 mm	0.12	1.14	0.42	0.94	1.18	0.26
RTI ¹⁾	0.91	1.16	0.55	0.70	0.79	0.95	1.10	1.23
Tibia Fz	5.2 kN	6.8 kN	3.14	3.97	3.40	5.94	3.75	7.00
Xversion	-	35 deg	-11.07	36.44	-12.74	24.72	-19.16	26.75
Dorsiflexion	-	35 deg	-42.11	-5.85	-42.02	-7.40	-50.39	-21.31

H III	Injury Limits	Case #1		Case #2		Case #3	
		Left	Right	Left	Right	Left	Right
Femur Fz	9.07 kN	-1.22	2.37	-1.34	2.84	-1.66	3.21
Knee Shear	15 mm	-0.12	0.14	1.31	0.19	0.29	0.27
TI ²⁾	1	0.42	0.73	1.23	1.99	1.77	3.13
Tibia Fz	8 kN	1.77	3.19	2.79	5.70	2.96	8.56

1) RTI: Revised Tibia Index, 2) TI: Tibia Index

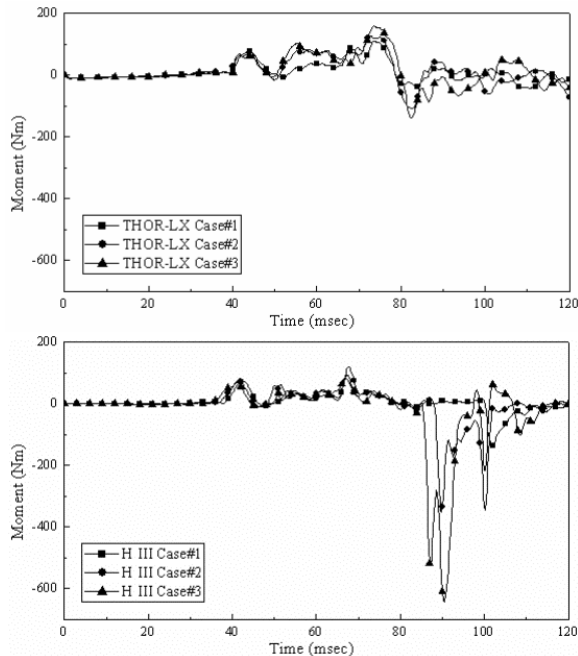


Fig. 22 Comparison of lower tibia dorsiflexion bending moments between Thor-Lx and Hybrid III

The behavior of the lower extremities of Thor-Lx, and Hybrid III for case #3 in the parameter study is depicted in Fig. 23.

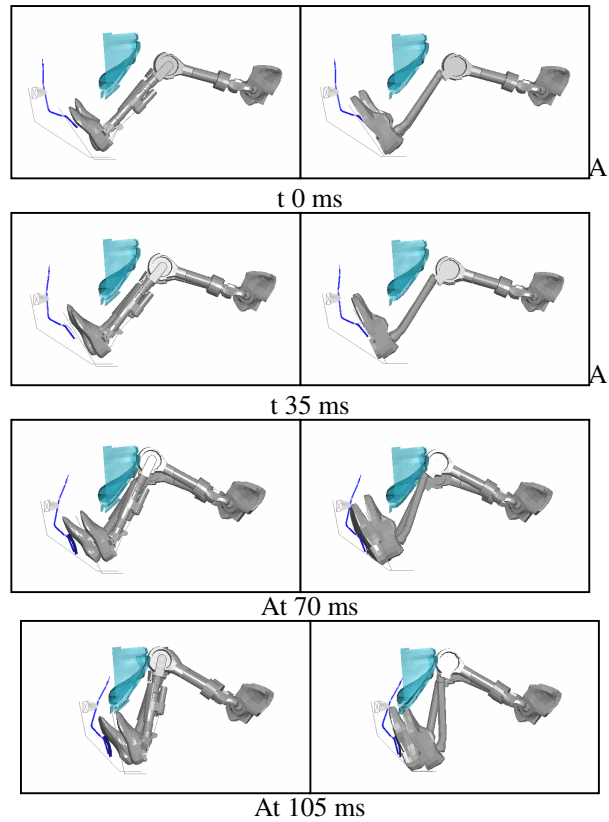


Fig. 23 Simulated lower extremity behaviors (Flesh has been made invisible, Left: Thor-Lx, Right: Hybrid III)

CONCLUSIONS

A finite element model of Thor-Lx has been completed. The model is computationally efficient since most non-deformable parts are modeled as rigid bodies, but it still successfully exhibited a good performance in the validation process. The modeling effort for the unique design of the ankle joints, which have two stages of moment-rotation characteristics, was made by employing kinematic joint elements together with definitions of sliding contact interface between the deformable rubber stoppers and rotating center blocks. This attempted to reproduce the hysteretic energy loss even for the multiple loading and unloading cycles.

In order to demonstrate the practical use of the model, a numerical investigation of lower leg injury risk from 40% offset crashes was performed. The comparative analysis with a Hybrid III dummy model showed that the use of Thor-Lx appears to be more favorable when assessing the lower leg injury risks due to its improved biofidelic design.

ACKNOWLEDGMENT

The authors would like to thank the NTBRC of NHTSA for providing the information of Thor dummy through their internet website. The authors also would like to thank Dr. Rodney Rudd at Center for Applied Biomechanics of UVA for reviewing the manuscript and providing a constructive commentary.

REFERENCES

- [1] National Automotive Sampling System-Crashworthiness Data System, 1994–1996, U.S. Department of Transportation, National Highway Traffic Safety Administration.
- [2] Morgan, R., et al. 1991. “Ankle Joint Injury Mechanism for Adults in Frontal Automotive Impact,” Proceedings of the 35th Stapp Conference
- [3] Kuppala, S., et al., “Lower Extremity Injuries and Associated Injury Criteria,” Seventeenth International Technical Conference on the Enhanced Safety of Vehicles, Amsterdam, June, 2001.
- [4] Tariq Shams. 2004. Presentation of Thor-NT: Features and Performance, SAE Thor Evaluation Task Group, Nashville, November 3rd
- [5] CATIA, VERSION 5, RELEASE 7, DASSAULT, FRANCE
- [6] HYPER-MESH, TRAINING MANUAL, VERSION 7.0, ALTAIR ENGINEERING. INC, USA
- [7] PAM-CRASH/SAFE USERS AND THEORY MANUAL, VERSION 2004, ESI GROUP, FRANCE
- [8] GESAC, “BIOMECHANICAL RESPONSE REQUIREMENTS OF THE THOR NHTSA ADVANCED FRONTAL DUMMY (Revision 2001.02)”
- [9] NHTSA VRTC, “CERTIFICATION PROCEDURE FOR THE THOR-LX/HYBRID III RETROFIT VERSION 3.2 October 2001”